



Low-dimensional modeling of hillslope subsurface flow: Relationship between rainfall, recharge, and unsaturated storage dynamics

A. G. J. Hilberts,^{1,2} P. A. Troch,^{1,3} C. Paniconi,⁴ and J. Boll⁵

Received 11 February 2006; revised 1 November 2006; accepted 24 November 2006; published 31 March 2007.

[1] We present a coupling between the one-dimensional Richards equation for vertical unsaturated flow and the one-dimensional hillslope-storage Boussinesq equation (HSB) for lateral saturated flow along complex hillslopes. Here the capillary fringe is included in the flow domain as an integral part of the Boussinesq aquifer. The coupling allows quantitative investigation of the role of unsaturated storage in the relationship between rainfall and recharge. The coupled model (HSB coupled) is compared to the original HSB model (HSB original) and a three-dimensional Richards equation (RE) based model (taken to be the benchmark) on a set of seven synthetic hillslopes, ranging from convergent to divergent. Using HSB original, the water tables are overestimated and the outflow rates are generally underestimated, and there is no delay between rainfall and recharge. The coupled model, however, shows a remarkably good match with the RE model in terms of outflow rates, and the delay between rainfall and recharge is captured well. We also see a clear improvement in the match to the water tables, even though the values are still overestimated for some hillslope shapes, in particular the convergent slopes. We show that for the hillslope configurations and scenarios examined in this paper it is possible to reproduce hydrographs and water table dynamics with a good degree of accuracy using a low-dimensional hydrological model.

Citation: Hilberts, A. G. J., P. A. Troch, C. Paniconi, and J. Boll (2007), Low-dimensional modeling of hillslope subsurface flow: Relationship between rainfall, recharge, and unsaturated storage dynamics, *Water Resour. Res.*, 43, W03445, doi:10.1029/2006WR004964.

1. Introduction

[2] Our understanding of hillslope subsurface flow processes and their effect on catchment response to atmospheric forcing is incomplete and has been the subject of much research for several decades. Among the first to reveal the importance of hillslope subsurface flow with regard to catchment stormflow were *Hewlett and Hibbert* [1967] and *Dunne and Black* [1970]. They concluded that for humid climates water table dynamics in hillslopes have a large effect on channel stormflow through the formation of areas of saturation along the channel network, often called saturated source areas, which cause saturation excess overland flow. Since then many studies have investigated subsurface flow processes experimentally [e.g., *O'Loughlin*, 1981; *Woods et al.*, 1997; *Torres et al.*, 1998; *McGlynn et*

al., 2004] and through modeling. The two-part paper by *Freeze* [1972], where stormflow processes are examined using a three-dimensional Richards-based model to describe subsurface processes, is one of the first (computer) modeling studies of hillslope processes, and since then many have followed.

[3] In addition to the rather complex, three-dimensional models that are often used in these modeling studies [e.g., *Abbott et al.*, 1986; *Wigmosta et al.*, 1994], several simplified low-dimensional models have been proposed, because of the computational expense and parameterization difficulties associated with the former type of model. Efforts include those of *Beven and Kirkby* [1979], who describe the original version of TOPMODEL, *Duffy* [1996], who develops a two-state variable integral-balance (hillslope) model, *Reggiani et al.* [1998], who describe the “representative elementary watershed” (REW) model, and *Sloan* [2000], who describes a storage-discharge type model which is derived from hydraulic groundwater theory. Among the simplified models, many studies have focused on analysis of the Boussinesq equation [e.g., *Childs*, 1971; *Brutsaert*, 1994; *Szilagyi et al.*, 1998; *Chapman*, 2005]. Most of these studies were conducted on straight hillslopes, sometimes using linearized versions of the Boussinesq equation, aiming at an increased fundamental understanding of the flow and storage dynamics in hillslopes.

[4] In recent work by the authors, the Boussinesq equation was generalized to account for the three-dimensional

¹Hydrology and Quantitative Water Management Group, Wageningen University, Wageningen, Netherlands.

²Now at Climate Hazard Model Development, Risk Management Solutions Ltd., London, UK.

³Now at Department of Hydrology and Water Resources, University of Arizona, Tucson, Arizona, USA.

⁴Centre Eau, Terre et Environnement, Institut National de la Recherche Scientifique, Université du Québec, Québec, Canada.

⁵Department of Biological and Agricultural Engineering, University of Idaho, Moscow, Idaho, USA.

soil mantle in which the flow processes take place [Troch *et al.*, 2003; Paniconi *et al.*, 2003; Hilberts *et al.*, 2004]. The effect of slope shape (i.e., convergent, divergent, and straight) and bedrock curvature on storage and outflow processes was examined for drainage and recharge scenarios, and compared to the three-dimensional Richards equation (RE) based model of Paniconi and Putti [1994]. A general conclusion of our recent work with the hillslope-storage Boussinesq (HSB) model is that the modeled outflow rates compared relatively well to results of the RE model, but capturing the water table dynamics was less successful. Results from a recent laboratory experiment [Hilberts *et al.*, 2005] indicated that this may be caused by the strong effect of capillarity (or, more precisely, the unsaturated storage) on groundwater dynamics, especially for shallow soils as typically encountered on hillslopes.

[5] The capillary fringe is an (almost) entirely saturated transition zone between the unsaturated zone and groundwater, of which the effects on groundwater flow are often ignored. However, the literature provides evidence that in the capillary fringe, fluxes can have considerable lateral components, thereby adding to lateral groundwater flow [e.g., Luthin and Miller, 1953; Jayatilaka and Gillham, 1996]. These flow processes were investigated numerically [e.g., Luthin and Day, 1955; Vachaud and Vauclin, 1975] and experimentally [e.g., Berkowitz *et al.*, 2004], and all of these studies clearly show large lateral flow components in the capillary fringe. Vachaud and Vauclin [1975] demonstrated that the fluxes in the capillary fringe are of the same order of magnitude as groundwater fluxes, and that they often have a large lateral component. They estimated that, for their experiment, roughly 14% of the lateral flux takes place above the water table.

[6] The effect of capillarity on water table dynamics, which in hydraulic groundwater models is usually accounted for through parameters such as specific yield, effective porosity, or drainable porosity, has been noted by Hooghoudt [1947], who referred to it as the “Wieringermeer effect,” and later by Gillham [1984], Abdul and Gillham [1989], Parlange *et al.* [1990], Kim and Bierkens [1995], and Nielsen and Perrochet [2000]. However, only few have tried to account for the effect. In a benchmark paper by Parlange and Brutsaert [1987] the capillarity effect on groundwater systems is modeled, assuming a deep profile for which $\theta = \theta_s$ holds at the land surface. Assuming instantaneous equilibrium in the unsaturated zone, an analytical expression to account for capillarity effects is derived that can be added to the Boussinesq equation. Barry *et al.* [1996] extended the equations derived by Parlange and Brutsaert [1987] to include higher-order capillarity effects, and they are used to investigate the inland propagation of oscillations in water tables for a coastal aquifer. Nachabe [2002] derives an analytical expression to account for dynamic capillarity effects, which also includes delayed recharge due to rapidly dropping water tables. Hilberts *et al.* [2005] derived an analytical expression to account for capillarity effects under equilibrium in shallow groundwater systems, and its influence on hillslope dynamics is investigated. All of these studies are mainly applicable in situations where recharge is negligibly small. To extend the investigation of the effect of unsaturated zone storage on saturated flow to

recharge scenarios, a coupling of the saturated zone model to a dynamic unsaturated zone model is needed, and the impact of the capillary fringe on water table dynamics needs to be incorporated.

[7] Hydrological studies at the hillslope and catchment scale, as well as land surface modeling, have put much emphasis on the processes that occur in the soil layer close to the soil surface. This is because the interactions of the unsaturated zone with the atmospheric boundary layer are known to have an important effect on surface fluxes and therefore also on climate [Koster *et al.*, 2003]. It is well known that subsurface flow processes are currently not well simulated in land surface models [Liang *et al.*, 2003]. A more thorough understanding of the interactions between (shallow) groundwater and soil moisture in the unsaturated zone is needed if we are to improve model results significantly [Koster *et al.*, 2000].

[8] Several authors have described a coupling of separate models for unsaturated and saturated flow under a diversity of assumptions. Pikul *et al.* [1974] coupled a one-dimensional Boussinesq model to a one-dimensional RE model for the unsaturated zone. The coupled system was solved as a boundary value problem, and the drainable porosity for the saturated zone model was taken to be a constant (namely, $\theta_s - \theta_m$), where θ_s (dimensionless) is saturated soil moisture content and θ_m (dimensionless) is “the minimum soil moisture content below the depth from which moisture may be removed directly by evapotranspiration.” As no functional form is given for θ_m , its value is somewhat arbitrary [Vachaud and Vauclin, 1975]. A very similar approach was used by Kim *et al.* [1999], but they also did not give a relationship describing the drainable porosity. Smith and Hebbert [1983] coupled a Boussinesq model to a kinematic wave model for the unsaturated zone. To calculate the recharge from the unsaturated zone to the saturated zone, they assumed that the soil moisture pulses in the unsaturated zone have attenuated when they reach the groundwater table. The coupled system was solved as a system of ordinary differential equations. A similar approach was taken by Beven [1982]; however, in his work, two kinematic wave models were coupled. Liang *et al.* [2003] described a coupling between a one-dimensional RE model for the unsaturated zone and a generalized bucket model for lateral subsurface flow, which was linked to the VIC model [Wood *et al.*, 1992]. The coupled system was also solved as a boundary value problem. However, in none of the mentioned papers that deal with coupling of models, the actual functional interactions between the saturated zone and the unsaturated zone are investigated.

[9] In this work the one-dimensional Richards equation is coupled to the HSB equation. In the coupled model, the capillary fringe is treated as an integral part of a Boussinesq aquifer, i.e., lateral groundwater transport takes place over the entire saturated depth (and not only below the atmospheric pressure plane). By introducing the unsaturated zone matric pressure head as a system state and reformulating the derived equations in state-space notation, we solve the coupled system simultaneously as a set of ordinary differential equations, and obtain a functional state-dependent expression for the drainable porosity. With a Richards equation representation for the unsaturated zone and a functional form for the drainable porosity, this coupled

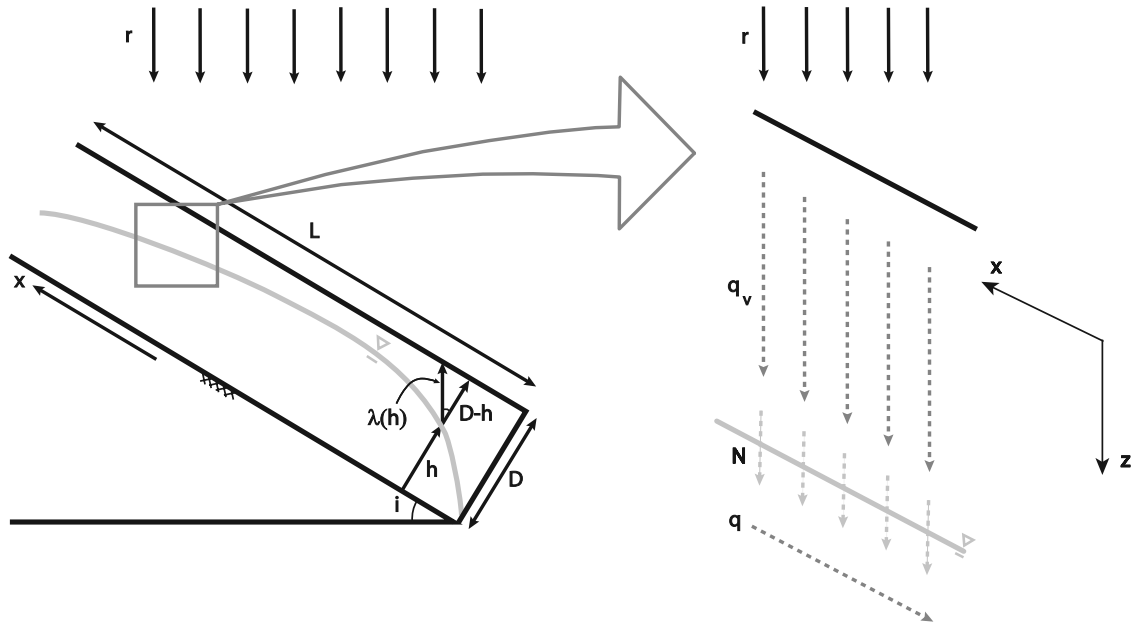


Figure 1. Definition sketch showing a hillslope cross section with relevant parameters and the coordinate systems for the unsaturated zone (vertical flow) and saturated zone (lateral flow).

model allows us to investigate more accurately the interactions between the saturated and unsaturated zone and the relationship between rainfall intensity, unsaturated storage (and drainable porosity), and recharge. We assume that a single (space-averaged) soil moisture profile can sufficiently describe the unsaturated zone processes, which is an assumption that is done to retain the coupled model's low dimensionality. A similar assumption underlies the work of *Boussinesq* [1877], where recharge was assumed uniform over a hillslope. The coupled HSB model's behavior is compared to the original HSB model of *Troch et al.* [2003] and the three-dimensional RE model of *Paniconi and Putti* [1994] (which is taken to be a benchmark model) for a set of seven synthetic hillslopes.

2. Governing Equations

2.1. Unsaturated and Saturated Zone of the Coupled Model

[10] If we assume that the soil water movement in the unsaturated zone is predominantly vertical, it can be described using the one-dimensional Richards equation:

$$\frac{\partial \theta}{\partial t} = \frac{d\theta}{d\psi} \cdot \frac{\partial \psi}{\partial t} = \frac{\partial q_v}{\partial z} \quad (1)$$

where $\theta = \theta(x, z, t)$ (dimensionless) is the volumetric soil moisture content, $\psi = \psi(x, z, t)$ [L] is the matric pressure, t is time, z is the vertical coordinate, positive downward (see Figure 1), and q_v is the vertical soil moisture flux [L/T], expressed as

$$q_v(z, t) = -K(\psi) \left(-\frac{\partial \psi}{\partial z} + 1 \right) \quad (2)$$

where $K(\psi)$ [L/T] is the hydraulic conductivity as a function of matric pressure. To describe $\theta(\psi)$ and $K(\psi)$, we use the *van Genuchten* [1980] relationships:

$$\theta(\psi) = \theta_r + (\theta_s - \theta_r) \left(\frac{1}{1 + (\alpha\psi)^n} \right)^m \quad (3)$$

$$K(\psi) = k \frac{\left(-1 + \left(1 - \left((1 + (\alpha\psi)^n)^{-m} \right)^{m-1} \right)^m \right)^2}{(1 + (\alpha\psi)^n)^{m/2}} \quad (4)$$

where k [L/T] is the saturated hydraulic conductivity, θ_r (dimensionless) is the residual soil moisture content, n (dimensionless), m (dimensionless), and α [1/L] are fitting parameters, and $m = 1 - 1/n$. To integrate the soil water retention curve, an alternate parameterization is more convenient:

$$\theta(\psi) = \theta_r + (\theta_s - \theta_r) \left(\frac{1}{1 + (\alpha'\psi)^{n'}} \right)^{m'} \quad (5)$$

where n' , m' , and α' are again fitting parameters, and $m' = 1 + 1/n'$ (see *Troch* [1992] and *Hilberts et al.* [2005]). Both parameterizations of the unsaturated zone are used in our modeling approach. The conventional parameterization is used to describe the relationships between pressure head, soil moisture content, and hydraulic conductivity for Richards' equation, whereas the alternate parameterization in a later stage is used to determine the value for the state-dependent drainable porosity (see section 2.2). Note that a single parameterization does not suffice in this modeling approach: the conventional parameterization is required to determine the unsaturated hydraulic conductivity and pressure head (using (4)), and the alternate parameterization is required to determine the drainable porosity in a later stage (using (20)).

[11] The saturated zone dynamics are modeled with the HSB model [Troch *et al.*, 2003; Paniconi *et al.*, 2003; Hilberts *et al.*, 2004]:

$$w\gamma \frac{\partial h}{\partial t} = -\frac{\partial(wq)}{\partial x} + N \cos(i)w \quad (6)$$

where $w = w(x)$ [L] is the hillslope width at x [L] running along the bedrock slope (positive in the upslope direction), γ (dimensionless) is the drainable porosity, $h = h(x, t)$ [L] is the water table height perpendicular to the bedrock, t [T] is time, $N = N(x, t)$ [L/T] is the vertical recharge to the groundwater table, and $q = q(x, t)$ [L²/T] is the lateral Darcy flux which is assumed to be parallel to the bedrock (i.e., Dupuit-Forchheimer assumption):

$$q(x, t) = -kh \left(\frac{\partial h}{\partial x} \cos(i) + \sin(i) \right) \quad (7)$$

where $i = i(x)$ (dimensionless) is the bedrock slope. In Figure 1 both the hillslope coordinate system and the vertical coordinate system are depicted.

2.2. Interactions Between the Saturated and the Unsaturated Zone

[12] Using the unsaturated zone model, it is possible to calculate the recharge N based on the position of the water table and the actual soil moisture profile. Mass conservation requires that for each location on the hillslope the following relationship holds

$$N(x, t) = r(t) - \frac{\partial}{\partial t} \left(\int_0^{\frac{(D-h)}{\cos(i)}} (\theta(x, z, t) - \theta_r) dz \right) \quad (8)$$

where D [L] is the soil depth and $r(t)$ [L/T] and $N(x, t)$ [L/T] are the vertical rainfall rate and recharge rate, respectively. Note that all terms in (8), including the integration boundaries, are in vertical coordinates. Chapman [2005] argued that although many studies use rainfall and recharge rates perpendicular to the bedrock, it is more realistic to consider the vertical fluxes. Furthermore, Chapman [2005] shows that both approaches yield similar results in terms of average water table height as long as the recharge/conductivity ratio is relatively small.

[13] For notational convenience we will use

$$\lambda(h) = \frac{(D-h)}{\cos(i)} \quad (9)$$

to indicate the depth to the water table in the vertical coordinate. Equation (8) can then also be formulated as

$$N(x, t) = r(t) - \left(\frac{\partial}{\partial t} \left(\int_0^\lambda (\theta_e(x, z, t) - \theta_r) dz \right) + \frac{\partial}{\partial t} \left(\int_0^\lambda (\theta(x, z, t) - \theta_e(x, z, t)) dz \right) \right) \quad (10)$$

where $\theta_e(x, z, t)$ is the soil moisture profile under hydraulic equilibrium conditions at t for a given water table position

and zero recharge. The changes in unsaturated storage are now expressed as storage changes relative to the hydraulic equilibrium storage profiles. This is done to avoid a singularity in the coupled model, as will be explained in section 2.4. Equation (10) can be written as

$$N(x, t) = r(t) - \left[\frac{\partial h'}{\partial t} \frac{d}{dh'} \left(\int_0^\lambda (\theta_e(x, z, t) - \theta_r) dz \right) + \frac{\partial}{\partial t} \left(\int_0^\lambda (\theta(x, z, t) - \theta_e(x, z, t)) dz \right) \right] \quad (11)$$

where $h' = h/\cos(i)$ is the vertical water table height above the bedrock. Because $\partial h'/\partial t = 1/\cos(i) \partial h/\partial t$, and $d/dh' = \cos(i) d/dh$, (11) is equivalent to:

$$N(x, t) = r(t) - \frac{\partial h}{\partial t} \frac{d}{dh} \left(\int_0^\lambda (\theta_e(x, z, t) - \theta_r) dz \right) - \frac{\partial}{\partial t} \left(\int_0^\lambda (\theta(x, z, t) - \theta_e(x, z, t)) dz \right) \quad (12)$$

[14] The term $d/dh (\int_0^\lambda (\theta_e(x, z, t) - \theta_r) dz)$ is the change of storage in the unsaturated zone (in hydraulic equilibrium) with respect to a change in water table height, which Hilberts *et al.* [2005] denoted as $-ds_1/dh$ and for which an analytical expression was derived:

$$\frac{d}{dh} \left(\int_0^\lambda (\theta_e(x, z, t) - \theta_r) dz \right) = -(\theta_s - \theta_r) \left(1 + (-\alpha' \lambda)^{n'} \right)^{-\frac{(n'+1)}{n'}} \quad (13)$$

where α' and n' are modified van Genuchten parameters defined by (5).

[15] The second term within the square brackets in (11) can be expanded by applying Leibniz' rule:

$$\begin{aligned} \frac{\partial}{\partial t} \left(\int_0^\lambda (\theta(x, z, t) - \theta_e(x, z, t)) dz \right) &= -\frac{1}{\cos(i)} \frac{\partial h}{\partial t} \cdot (\theta(x, \lambda, t) - \theta_e(x, \lambda, t)) \\ &+ \int_0^\lambda \frac{\partial \theta}{\partial t} dz - \int_0^\lambda \frac{\partial \theta_e}{\partial t} dz \end{aligned} \quad (14)$$

Note that both the equilibrium and the actual soil moisture content are at full saturation at the position of the water table (i.e., $\theta(x, \lambda, t) = \theta_e(x, \lambda, t) = \theta_s$), which allows (14) to be further reduced. The changes in the equilibrium profile depend directly on the changes in water table height (i.e., the profile is displaced according to the displacement of the water table):

$$\begin{aligned} \int_0^\lambda \frac{\partial \theta_e(x, z, t)}{\partial t} dz &= \int_0^\lambda \frac{d\theta}{d\psi} \frac{\partial \psi_e(x, z, t)}{\partial t} dz \\ &= \int_0^\lambda \frac{d\theta}{d\psi} \frac{\partial h'(x, t)}{\partial t} dz \\ &= \frac{1}{\cos(i)} \int_0^\lambda \frac{d\theta}{d\psi} \frac{\partial h(x, t)}{\partial t} dz \end{aligned} \quad (15)$$

where ψ_e is the equilibrium pressure head. Upon combination of (12), (13), (14), and (15), equation (8) becomes

$$N(x, t) = r(t) + \frac{\partial h}{\partial t} (\theta_s - \theta_r) \left(1 + (-\alpha' \lambda)^{n'} \right)^{-\left(\frac{d+1}{n'}\right)} - \int_0^\lambda \frac{\partial \theta}{\partial t} dz + \frac{1}{\cos(i)} \int_0^\lambda \frac{d\theta}{d\psi} \frac{\partial h}{\partial t} dz \quad (16)$$

For a Boussinesq-type aquifer (i.e., without any retention effects of the unsaturated zone), the drainable porosity parameter in (6) is a constant

$$\gamma = (\theta_s - \theta_r) \quad (17)$$

Substitution of (16) and (17) into (6) yields the expression for the saturated zone model, and taking the derivative of (2) with respect to z and substituting this into (1) yields the unsaturated zone model. Together these form a coupled system with a state-dependent drainable porosity, without inclusion of the capillary fringe in the Boussinesq flow domain:

$$wf \frac{\partial h}{\partial t} = -\frac{\partial(wq)}{\partial x} + w \left\{ r - \int_0^\lambda \frac{\partial \theta}{\partial t} dz + \frac{1}{\cos(i)} \int_0^\lambda \frac{d\theta}{d\psi} \frac{\partial h}{\partial t} dz \right\} \cdot \cos(i) \quad (18)$$

$$C \frac{\partial \psi}{\partial t} = -\frac{\partial K(\psi)}{\partial z} \left(1 - \frac{\partial \psi}{\partial z} \right) + K(\psi) \frac{\partial^2 \psi}{\partial z^2} \quad (19)$$

where $f = f(h)$ is the drainable porosity after *Hilberts et al.* [2005], modified such that recharge rate is vertical instead of perpendicular to bedrock:

$$f(h) = (\theta_s - \theta_r) \left\{ 1 - \cos(i) \left(1 + (-\alpha' \lambda)^{n'} \right)^{-\left(\frac{d+1}{n'}\right)} \right\} \quad (20)$$

and $C = C(\psi)$ is the differential moisture capacity:

$$C(\psi) = \frac{d\theta}{d\psi} \quad (21)$$

2.3. Governing Equations With Inclusion of the Capillary Fringe

[16] The conclusions of *Paniconi et al.* [2003] are that the high outflow rates and the relatively low water table values for the RE model compared to the HSB models indicate that the HSB models are draining too slowly. Given the findings from this study and the importance of the capillary fringe on lateral groundwater flow and water table dynamics as reported in the literature reviewed earlier, we will include the capillary fringe in our coupled model.

[17] When a capillary fringe ψ_c is introduced as an integral part of the aquifer, the governing equations for the coupled model are not greatly altered. If we define

$$h^* = h - \psi_c \quad (22)$$

to be the saturated depth over which lateral transport takes place [L], and we substitute this expression into (18) and (19), the equations essentially remain the same. In (18) the

integral boundary becomes $\lambda = (D - \bar{h})/\cos(\bar{i}) - \psi_c$, and equation (19) does not change. However, flow equation (7) changes to

$$q(x, t) = -kh^* \left(\frac{\partial h}{\partial x} \cos(i) + \sin(i) \right) \quad (23)$$

and the drainable porosity f (equation (20)) is now calculated based on the new value for λ .

[18] We will refer to the model based on (18), (19), and (23) as HSB coupled, and this model's behavior will be compared to the original HSB model and an RE based model.

[19] We will test the hypothesis that the term within accolades in (18) can be approximated using a single soil moisture profile derived for the entire hillslope, analogous to the assumption underlying the original work of *Boussinesq* [1877] that recharge is uniform. If this hypothesis leads to acceptable levels of accuracy, it allows for a significant reduction in the dimensionality of the model. This hypothesis implies that $\theta(x, z, t)$ is assumed equal for all x , and the integration over the profile $\theta(x, z, t)$ therefore is conducted using boundaries based on a hillslope-averaged water table height:

$$\lambda = \lambda(\bar{h}^*) = \frac{(D - \bar{h}^*)}{\cos(\bar{i})} \quad (24)$$

where

$$\bar{h}^*(t) = 1/(\bar{w}L) \int_0^L w(x)h^*(x, t) dx$$

$$\bar{i} = 1/(\bar{w}L) \int_0^L w(x)i(x) dx$$

$$\bar{w} = 1/L \int_0^L w(x) dx$$

where \bar{h}^* is the average height of the saturated zone (the capillary fringe included), \bar{w} is the average width, \bar{i} is the average bedrock slope, and L [L] is the hillslope length measured along the bedrock. By introducing a state vector $\mathbf{X} = [h(x, t), \psi(z, t)]$, and discretizing in the spatial coordinates z and x (see Figure 1), (18) and (19) can be solved simultaneously as a set of ordinary differential equations.

2.4. Alternate Derivation Involving Singularity

[20] The most obvious manner to expand (8) would be to directly regard soil moisture profile changes with respect to θ_r . Applying Leibniz' rule in this case yields:

$$N(x, t) = r(t) - \int_0^\lambda \left(\frac{\partial \theta(x, z, t)}{\partial t} \right) dz + \frac{\partial h}{\partial t} (\theta(x, \lambda, t) - \theta_r) \quad (25)$$

The third term on the right-hand side of (25) would normally be brought to the left-hand side, thereby altering the constant parameter γ in (6) to become a state-dependent parameter $f(h)$. However, since $\theta(x, \lambda, t) = \theta_s$, upon combination of (25) and (6) a singularity arises on the left-hand side of (6):

$$f = (\theta_s - \theta(x, \lambda, t)) \quad (26)$$

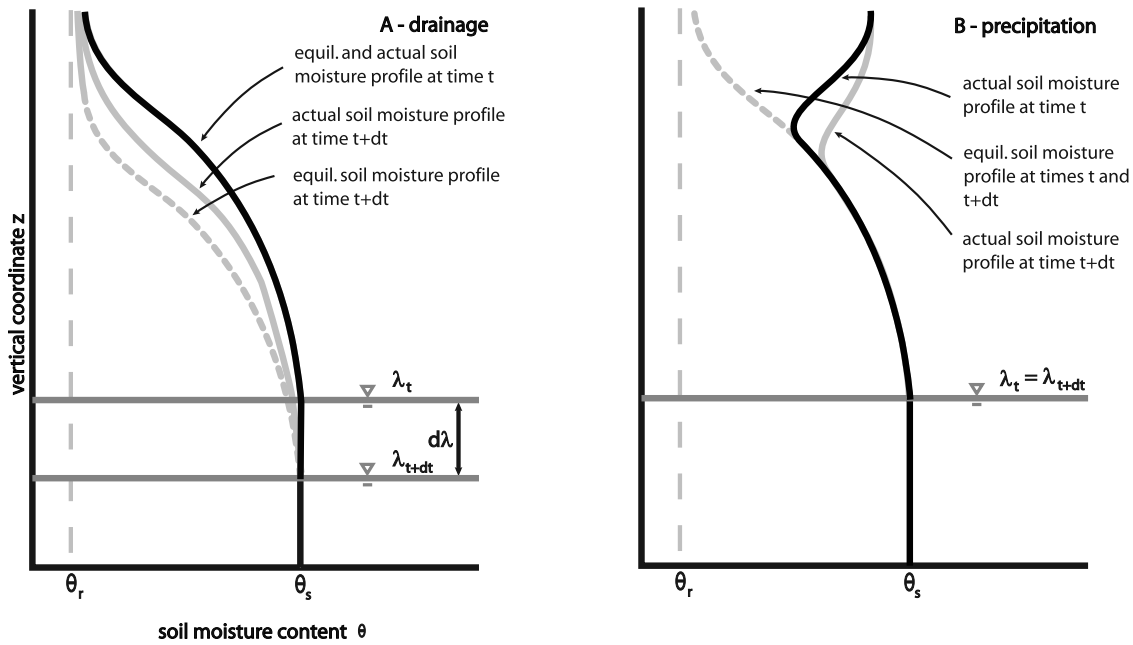


Figure 2. Sketch of soil moisture profile, and changes in soil moisture content for (a) a drainage and (b) a recharge scenario at times t and $t + dt$.

and since at the water table $\theta(x, \lambda, t) = \theta_s$, it causes a singularity in equation (6).

[21] In the derivation of section 2.2 this singularity is avoided by regarding the changes of soil water profile with respect to equilibrium profile, for which the drainable porosity is expressed analytically and subsequently corrected by an extra source term (namely, $\int_0^{\lambda} \frac{d\theta}{d\psi} \frac{\partial h}{\partial t} dz$) that accounts for changes in equilibrium profile.

2.5. Three-Dimensional Richards Equation Based Model

[22] The governing equation for the three-dimensional RE model is [Paniconi and Wood, 1993]:

$$\eta(\psi) \frac{\partial \psi}{\partial t} = \nabla \cdot (K(\psi)(\nabla \psi + \mathbf{e}_z)) \quad (27)$$

where $\eta = S_w S_s + \theta_s (dS_w/d\psi)$ is the general storage term, S_w is the water saturation defined as θ/θ_s , S_s is the aquifer specific storage coefficient, \mathbf{e}_z is the vector $(0,0,1)^T$ (positive upward), and the hydraulic conductivity tensor is $K(\psi)$ as in (4). The nonlinear retention characteristics are described using the van Genuchten relationship given in (3). The RE model used in this work is the subsurface module of a coupled surface-subsurface numerical model using a tetrahedral finite element discretization in space, a weighted finite difference scheme in time, and Newton or Picard iteration to resolve the nonlinearity [Paniconi and Putti, 1994; Putti and Paniconi, 2004].

3. Interpretation

3.1. Interpretation of the Equations for the Coupled Model

[23] In the coupled model (equation (16)) the unsaturated zone affects the water table dynamics in two distinct ways. First, the unsaturated zone replenishes the groundwater

(namely, the third and fourth terms on the right-hand side of (16)). These terms together indicate the total change in soil moisture storage for a certain depth to the water table λ . Second, the soil moisture profile in the unsaturated zone determines the available storage capacity in the soil above the water table, which is reflected in the second term on the right-hand side of (16), thereby directly influencing the drainable porosity.

[24] In Figure 2, hypothetical soil moisture profiles for times t and $t + dt$ (and corresponding depth to water table values $\lambda(\bar{h}(t))$ and $\lambda(\bar{h}(t + dt))$) are depicted for a drainage and a rainfall scenario. The solid lines give the actual soil moisture profiles (at two different times), the dashed lines are the equilibrium soil moisture profiles, the black lines correspond to the profiles at $t = t$, and the gray lines correspond to those at $t + dt$. For convenience let us name the term within accolades in (18):

$$N^*(x, t) = r(t) - \underbrace{\int_0^{\lambda} \frac{\partial \theta}{\partial t} dz}_{\text{actual}} + \underbrace{\frac{1}{\cos(i)} \int_0^{\lambda} \frac{d\theta}{d\psi} \frac{\partial h}{\partial t} dz}_{\text{equilibrium}} \quad (28)$$

For a drainage scenario (Figure 2a) starting from hydraulic equilibrium, the total change in actual soil moisture content (the second term on the right-hand side of (28)) is always equal to or greater (i.e., less negative) than the total change in equilibrium soil moisture storage (the third term). Note that because initially all the soil moisture changes will be negative for a drainage experiment, the absolute value of the second term will be smaller than the value of the third term. Therefore, for a short time at the onset of a drainage experiment, N^* will be negative. Later in the drainage process the water tables will drop more slowly and the unsaturated zone replenishes the saturated zone, causing N^* to become positive. The drainable porosity f (equation (20)) accounts for the changes in equilibrium profile and is smaller than $(\theta_s - \theta_r)$, and greater than zero. In the case

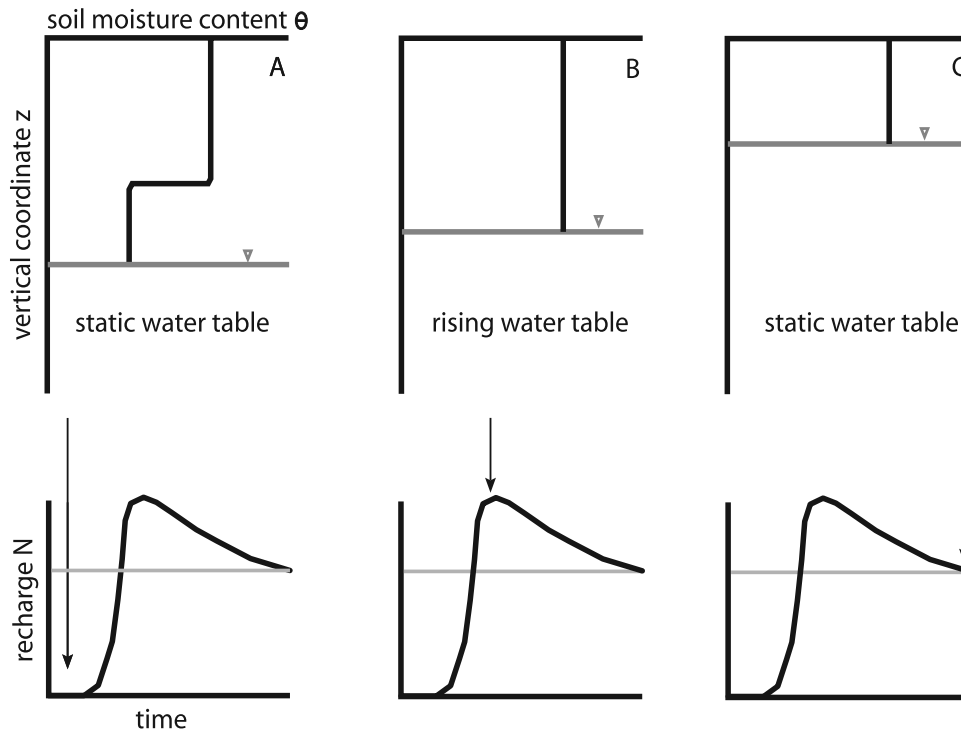


Figure 3. Schematic representation of the interactions between soil moisture dynamics (as a result of rainfall) and recharge rates (a) before, (b) during, and (c) after a soil moisture pulse reaches the water table.

where the actual profiles collapse into the equilibrium profiles N^* becomes zero, and the solution converges to the solution derived in *Hilberts et al.* [2005] but modified for vertical drainage.

[25] In the case of rainfall, the value and sign of N^* depends strongly on the water table height, the soil moisture conditions and the rainfall rate. When the water table is steady (i.e., $\lambda(\bar{h}(t)) = \lambda(\bar{h}(t + dt))$) and the unsaturated zone is initially relatively dry, most water from rainfall will be stored in the unsaturated zone. In (28) this means that the third term on the right-hand side becomes zero, the first and second term become equal, thereby causing N^* to be zero. When the unsaturated zone initially is relatively wet (Figure 2b), only part of the water coming from rainfall will be stored in the unsaturated zone, and the remainder will recharge the groundwater. In case the water table is dropping, and a soil moisture pulse is traveling toward the water table, a mix of the responses above will occur.

3.2. Relationship Between Rainfall, Recharge, and Unsaturated Storage

[26] The interaction between rainfall and recharge rates is illustrated in Figure 3, showing the (simplified) response of the unsaturated and saturated zones to a constant rainfall rate. We distinguish three stages: stage A, where a soil moisture wave due to rainfall is traveling toward a static water table in an initially relatively dry profile, stage B where the soil moisture pulse reaches the water table and causes the water table to rise, and stage C where the water table has reached a new equilibrium under recharge. In stage A all the rainwater that infiltrates is stored in the unsaturated zone and recharge is zero. Stage B shows the situation just

after the soil moisture front has reached the groundwater, causing a rapid rise in water table height. Note that during this stage of rising water tables, the recharge is higher than the rainfall rate. For a static water table, the flux across the water table surface would be equal to the rainfall rate, but since the water table is rising and thereby “taking up” water from the unsaturated zone, the recharge is higher than the rainfall rate. The phenomenon of the unsaturated and saturated zones competing for unsaturated storage just above the water table was also mentioned in studies such as *Duffy* [1996], *Seibert and McDonnell* [2002], and *Weiler and McDonnell* [2004]. When a new steady state water table position is reached (i.e., stage C), the water table is static, and the flux across it is equal to the rainfall rate.

[27] Since the increased recharge of stage B is due to movement of the water table $\partial h/\partial t$, and is therefore brought to the left-hand side of (6), the term determines the value of drainable porosity f . The second term on the right-hand side of (16) can thus be either regarded as an input term, or as a correction term for the storage coefficient γ in (6).

4. Model Comparison Setup

4.1. Models and Hillslopes

[28] We compare the coupled HSB (HSB coupled) model’s response to that of the three-dimensional Richards equation (RE) model described in section 2.5, and the original uncoupled HSB model (HSB original) described by *Troch et al.* [2003] and given by (6). The original HSB model is run in an uncalibrated mode assuming that the value of drainable porosity is $\gamma = (\theta_s - \theta_r)$, which can be considered a reasonable and conservative a priori estimate

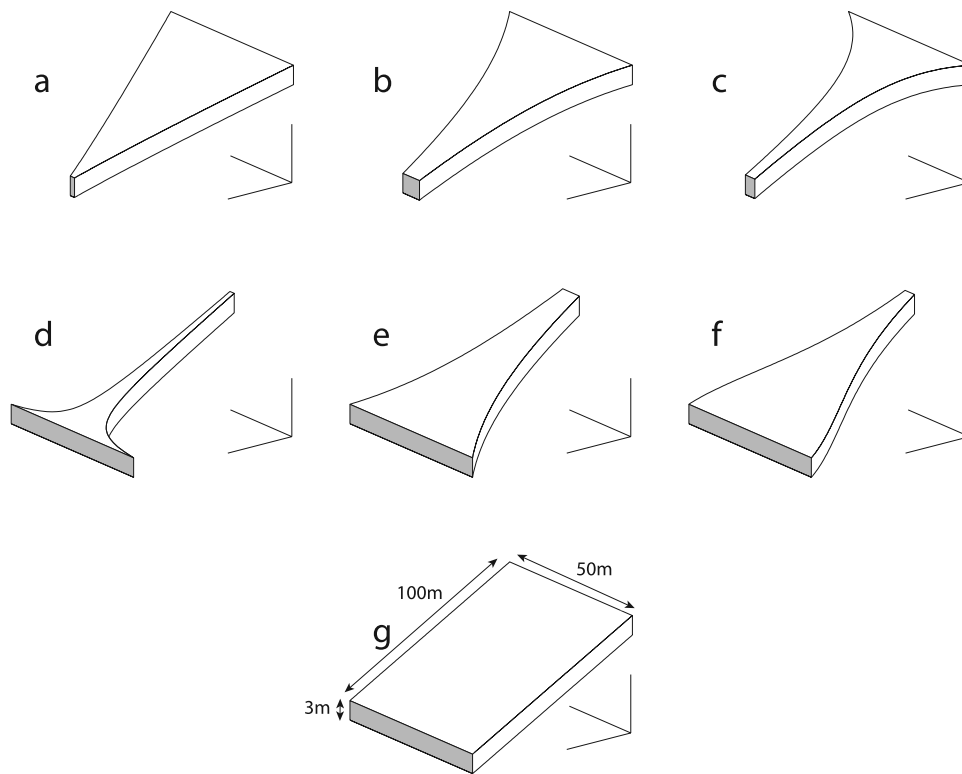


Figure 4. Three-dimensional view of (a, b, c) three convergent, (d, e, f) three divergent, and (g) a straight hillslope used in the model comparison study.

for a sandy soil when precise retention characteristics are unknown. Moreover, this is the value of γ one would obtain for a perfectly draining soil, which corresponds to a Boussinesq aquifer. We test the model's response under rainfall and during drainage on a set of seven artificial hillslopes that were also used by *Troch et al.* [2003], consisting of three convergent, three divergent, and one straight hillslope. The hillslope outlines are based on the nine geometries described by *Troch et al.* [2002] but have noncurved bedrock; thus the three straight slopes of *Troch et al.* [2002] collapse into a single slope, yielding seven hillslopes as depicted in Figure 4. The aquifer properties are given in section 4.3. The hillslopes have a length of 100 m and range in width from 50 m to 1.72 m. A sandy soil of 3 m depth overlies an impervious bedrock layer. On these hillslopes the models are compared under a constant rainfall intensity of 10 mm/d for the first 50 days, followed by a free drainage period.

[29] We use a sandy soil in our simulations since its properties correspond best with the original assumptions underlying Boussinesq's theory, which are 1) presence of a free surface (i.e., a sharp transition from saturated to dry aquifer material), and 2) bed-parallel flow lines in the saturated zone (i.e., the Dupuit-Forchheimer assumption). Moreover, in the process of coupling the models it is assumed that 3) the flow lines are predominantly vertical in the unsaturated zone and lateral in the saturated zone. All assumption becomes less valid for soils with a more gradual transition from the "wet" to "dry" part of the retention curve (e.g., loam or clay soils). A strongly capillary soil has no sharp transition from saturated to dry aquifer material (assumption 1). Moreover, a strongly capillary soil shows

an increasingly laterally directed flux as one moves toward the wetter end of the retention curve (i.e., toward the water table), which is in conflict with assumption 3. The importance of this phenomenon is also acknowledged by *Michiels et al.* [1989] and by *Berkowitz et al.* [2004], who state that in their experiments, complex distributions of soil moisture as well as horizontal flows are seen to occur both above and below the water table.

[30] If inclusion of capillarity effects leads to improved results for a sandy soil, we will have demonstrated the importance of unsaturated storage for a "worst-case" scenario. We thus expect even more noticeable effects for soil types with a larger capillary fringe (i.e., loam, clay), even though it then remains to be seen if the original assumptions underlying the work still prove valid for these soil types.

[31] The discretization is conducted such that, even though the unsaturated zone varies in depth, the vertical and lateral coordinates are both situated in a static frame of reference and discretized using a fixed number of nodes. The node spacing for the simulations in this work are $\Delta z = 0.075$ m and $\Delta x = 1$ m.

4.2. Boundary and Initial Conditions

[32] For the saturated zone, it is assumed that the downhill boundary condition is $h(0,t) = 0$, and the uphill boundary condition is a zero-flux boundary as are all sides and the bedrock. At the upper boundary of the unsaturated zone we assume that the flux across the soil surface is equal to the rainfall rate: $q_v(0, t) = r(t)$. At the lower boundary (i.e., the bedrock) the pressure head is equal to the average water table height $\psi(D/\cos(\bar{i}), t) = \bar{h}(t)/\cos(\bar{i})$ for the coupled HSB model.

Table 1. Van Genuchten Parameters (Conventional and Modified) for the Sandy Soil Used in the Comparison Study

Parameter	Sand	
	Conventional ^a	Modified ^b
θ_s	0.408	0.408
θ_r	0.054	0.054
α , 1/cm	-0.0254	-0.0081
n	1.9529	1.4154

^aFor conventional, $m = 1 - 1/n$.

^bFor modified, $m = 1 + 1/n$.

[33] The initial condition for all models is a uniform water table $h(x,0) = 0.10$ m above the bedrock, measured perpendicular to the bedrock for the coupled and original HSB models and vertical for the RE model, yielding comparable initial conditions (see *Paniconi et al.* [2003] for details). For HSB coupled and the RE model we furthermore assume that the initial condition in the unsaturated zone is that of vertical hydraulic equilibrium. This yields a positive pressure head at the bedrock $\psi(D/\cos(\bar{i}), t) = \bar{h}(t)/\cos(\bar{i})$ for HSB coupled, and $\psi(D/\cos(\bar{i}), t) = h(t)/\cos(\bar{i})$ for the RE model. The two formulations for the initial conditions differ slightly because HSB coupled uses a single unsaturated zone profile, whereas the RE model is fully three-dimensional.

4.3. Hillslope and Soil Parameters

[34] The hillslope plan shapes and dimensions are shown in Figure 4. For the simulations a bedrock slope of $i(x) = 5\%$ is used. The sandy soil overlaying the impervious bedrock has a saturated hydraulic conductivity of $k = 5$ m/d, and a aquifer specific storage coefficient $S_s = 0.01$ m⁻¹. Table 1 lists the van Genuchten parameters for the conventional parameterization (i.e., $m = 1 - 1/n$), and for the modified parameterization of *Troch* [1992] and *Hilberts et al.* [2005] (i.e., $m' = 1 + 1/n'$). The corresponding soil water retention characteristics are plotted in Figure 5.

4.4. Parameterization of the Capillary Fringe

[35] The capillary fringe is a narrow zone that serves as a transition between the vadose zone and the groundwater zone. The lower limit of the capillary fringe is commonly accepted to be the surface where pressure head is equal to zero, but the upper limit is scarcely definable [*Hillel*, 1980], with different authors placing it anywhere between 75% and 100% water saturation. *Berkowitz et al.* [2004] argued that the term “capillary fringe” should be replaced by the term “partially saturated fringe”, because just above (and below) the water table we often find small inclusions of entrapped air or inclusions of partially saturated soil causing the water content to be less than 100%. A range of ψ values for which $\theta(\psi)$ is “close” to θ_s therefore is a more appropriate definition [*Bear*, 1972]. For the soils in this study the capillary fringe (or partially saturated fringe) is defined as the lowest value of ψ for which the soil moisture value is higher than $0.85 \theta_s \simeq 0.35$, which corresponds to a capillary fringe $\psi_c \simeq -0.27$ m. The value is set at 85% water saturation because this is in good agreement with textbook values [e.g., *Bear*, 1972], and the resulting value for ψ_c is

also in the range of values for a sandy soil [e.g., *Harr*, 1962; *Bear*, 1972].

5. Model Comparison Results

5.1. Hydrographs and Water Tables

[36] We describe the results of the model runs using HSB coupled and we compare them with HSB original and the RE model.

[37] Figure 6 shows the outflow rates of the RE model, HSB original, and HSB coupled. The fit of the hydrographs of both HSB models compared to the RE model, for the rising and falling limb, is summarized in Table 2. From Figure 6, we notice that for short times after initiation of the experiment, HSB original shows higher fluxes than the RE model, which is due to the absence of an unsaturated zone description in this model, causing an instantaneous reaction to rainfall. This is most clearly visible for the divergent slopes (i.e., hillslopes d, e, f), where the hydrographs only climb after approximately 5–10 days for both the RE and the HSB coupled model, whereas the HSB original model shows an increase in flux starting at $t = 0$. At later times, however, the HSB original fluxes are generally underestimated. These findings are supported by the values of the mean absolute errors given in Table 2. We see that HSB original has higher mean absolute error values for all slopes in both the rising and falling limbs, with the exception of slope 3 (rising limb only) where due to a low estimation of the initial flux the errors for HSB original and HSB coupled are comparable.

[38] Comparing the hydrographs of HSB coupled and the RE model, we see a remarkably good agreement on all hillslopes. Also the timing of both hydrographs (i.e., the time at which the hydrograph starts to climb, and the time when peak outflow is reached) matches well. The goodness of fit suggests that a single soil moisture profile yields an adequate approximation of the unsaturated zone processes (as hypothesized in section 2.2) is accepted.

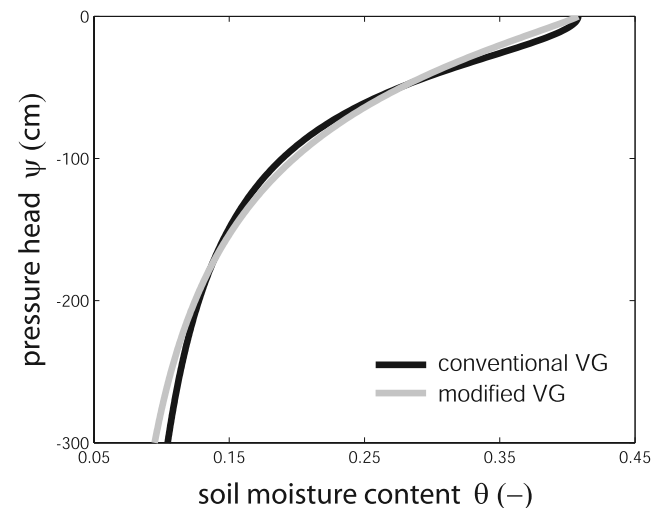


Figure 5. Retention characteristics of the sandy soil used in the model comparison. The black line depicts the conventional van Genuchten curve ($m = 1 - 1/n$), and the gray line is the modified van Genuchten curve ($m' = 1 + 1/n'$).

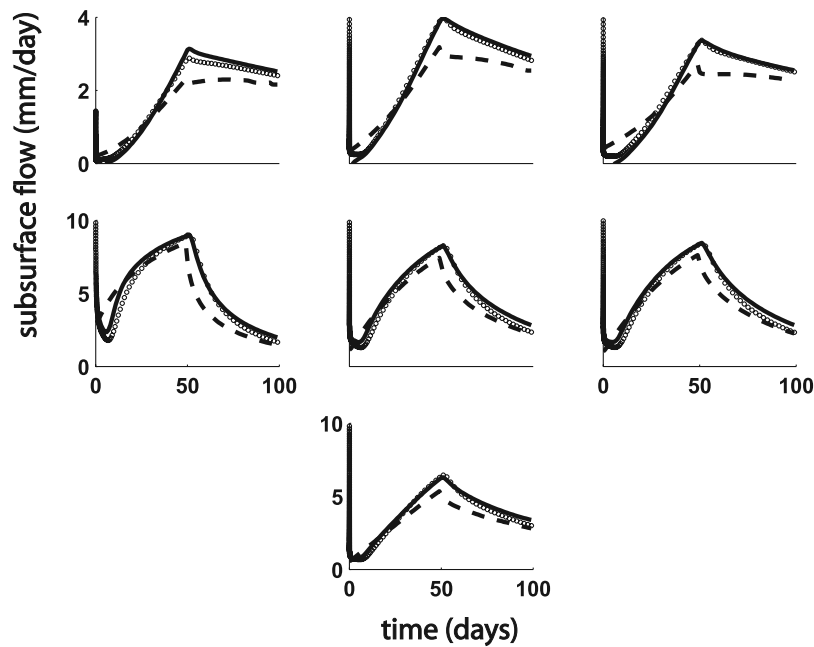


Figure 6. Outflow hydrographs as a result of a rainfall rate of 10 mm/d for the first 50 days followed by a pure drainage period for HSB coupled (solid lines), HSB original (dashed lines), and the RE model (circles).

[39] In Figure 7 the water tables are shown for HSB coupled, the RE model, and HSB original, after 5 days, 20 days, 50 days, and 100 days. Table 3 summarizes the mean absolute errors in the water table values for each of these times when compared to the benchmark RE model. The water tables after 5 days are remarkable: whereas HSB original is performing very poorly (i.e., large overestimation of water tables), the HSB coupled water tables match almost perfectly on all hillslopes; the modeled water tables are in many cases indistinguishable from the RE results. The water tables after 20 days also show a remarkable match for HSB coupled for all hillslopes. Looking at the results after 50 and 100 days, we see that both HSB models produce similar water table heights for the convergent slopes, with both models overestimating the water table heights. For the divergent slopes both models again overestimate the water table height, but the match for the HSB coupled model is much better than that of HSB original.

[40] Overall we conclude that HSB coupled is clearly better able to reproduce the hydrographs for all hillslopes, and in particular for the divergent slopes. The same holds for the water table values, except that the advantages of HSB coupled over HSB original for the convergent slopes at later times in the experiment is less noticeable. The differences between the HSB coupled and RE water table profiles, for the convergent slopes in particular, may be caused by errors introduced when using a single soil moisture profile for HSB coupled. We expect that this error will be largest for convergent slope shapes and steep slope angles, because of the relatively sharp gradients in water tables at later times in the experiment. The validity of using a single soil moisture profile for higher bedrock slopes and more convergent shapes will be investigated in future work, especially considering that overland flow may occur in these simulations, causing very different local responses.

5.2. Recharge Rates

[41] Figure 8 shows the value of the recharge term N in (16) and the rainfall rates during the experiment. We see that the values of N are initially negative due to a rapidly dropping water table and little water supply by the unsaturated zone. When the soil moisture front (due to rainfall) approaches the water table (roughly between $t = 2$ and $t = 4$ days), the value of N rises to positive values. The positive recharge rates cause the water tables to rise, thereby taking up water from the unsaturated zone, which in turn causes enhanced recharge rates (roughly between $t = 4$ and $t = 10$ days). As the water table rises, the lateral flux increases and (roughly around $t = 10$ days) the water table and outflow rate start to converge toward steady state. A new equilibrium is reached when $r = N$, which on the divergent hillslopes (d to f) is approached around $t = 50$ days. Because the rainfall rates drop to 0 mm/d at $t = 50$ days, the equilibrium is not fully reached. Just after $t = 50$ days we

Table 2. Mean Absolute Errors in the Hydrographs of HSB Original and HSB Coupled When Compared to the RE Model^a

	Slope						
	a	b	c	d	e	f	g
<i>Rising Limb Error</i>							
HSB original	0.23	0.36	0.33	0.80	0.58	0.56	0.54
HSB coupled	0.22	0.32	0.36	0.41	0.36	0.35	0.35
<i>Falling Limb Error</i>							
HSB original	0.38	0.51	0.44	1.00	0.66	0.61	0.62
HSB coupled	0.06	0.13	0.16	0.39	0.47	0.51	0.26

^aValues are in mm/d.

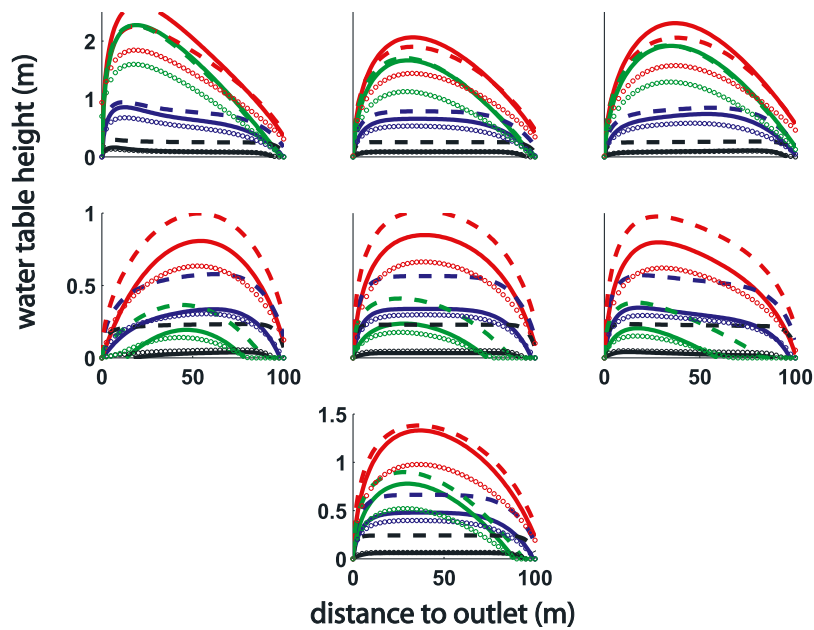


Figure 7. Water tables for HSB coupled (solid lines), HSB original (dashed lines), and the RE model (circles), after 5 (black), 20 (blue), 50 (red), and 100 days (green).

see that the recharge rates decline quickly, and eventually drop to below $N = 0$ due to the falling water tables.

6. Discussion

[42] In the Introduction we indicated that over the past decades there have been many attempts to model hillslope and catchment hydrological processes. Most of these attempts have been aimed at predicting outflow rates, but recently several model studies have also investigated the water table dynamics (or saturated storage dynamics) that are of crucial importance in determining the location and size of variable source areas, and thereby also to assess the risk for flood peaks in the channel network draining a hillslope or catchment. Examples include work by *Wigmosta et al.* [1994] and *Ivanov et al.* [2004], who present high-dimensional catchment-scale models, and *Seibert and McDonnell* [2002], *Weiler and McDonnell* [2004], and *Brooks et al.* [2007] who present the results of a conceptual modeling study applied to the hillslope scale. Even though these models have been applied successfully in the studies presented, they are all partly or fully conceptual instead of physically based, which makes the investigation of the exact interactions between the saturated and unsaturated zones cumbersome. In this work we have presented a physically based low-dimensional hillslope model. In the test cases we assumed that the conductivity, soil depth and other soil properties are constant in depth and in the direction along the hillslope, but the saturated module of the coupled model and the original HSB model are capable of handling spatial variability along these axes. On the other hand, since all variables and properties are assumed to be constant over the width of the hillslope, we cannot account for spatial variability along this axis. In the current version of the coupled formulation we also cannot account for spatial variability in rainfall rate or soil hydraulic properties of the unsaturated zone, because a single soil moisture profile

is used to model the unsaturated zone dynamics. Moreover, we assume that groundwater fluxes are parallel to the bedrock, and we do not use an infiltration model, thus the rainfall is assumed to infiltrate fully into the soil column (i.e., no infiltration excess runoff).

[43] The properties of the sandy soil in our simulations correspond best with the original assumptions underlying Boussinesq's theory, as the equations were derived for highly conductive and relatively shallow soils. Also the assumption of vertical flow in the unsaturated zone and lateral flow in the saturated zone correspond best to a soil with a quick transition from "wet" to "dry" in the soil water retention curve. Sandy soils have a smaller capillarity effect than silt, loam or clay soils. Hence the improvement in hydrological simulations when coupling the saturated and unsaturated zones presented here, provides a good test case in terms of saturated properties and retention characteristics. For less conductive soils, we expect greater improvement when including the capillarity effects than achieved for the sandy soil type. However, we should note that as the effects

Table 3. Mean Absolute Errors in the Water Tables of HSB Original and HSB Coupled When Compared to the RE Model^a

Model	Time, days	Slope						
		a	b	c	d	e	f	g
HSB original	5	0.16	0.17	0.17	0.18	0.18	0.18	0.17
HSB coupled	5	0.01	0.01	0.01	0.02	0.01	0.01	0.01
HSB original	20	0.26	0.26	0.26	0.25	0.26	0.26	0.26
HSB coupled	20	0.06	0.05	0.06	0.02	0.01	0.02	0.03
HSB original	50	0.34	0.37	0.39	0.30	0.31	0.30	0.35
HSB coupled	50	0.29	0.27	0.32	0.09	0.09	0.08	0.16
HSB original	100	0.40	0.39	0.44	0.15	0.16	0.14	0.26
HSB coupled	100	0.35	0.31	0.36	0.07	0.08	0.09	0.17

^aValues are in m.

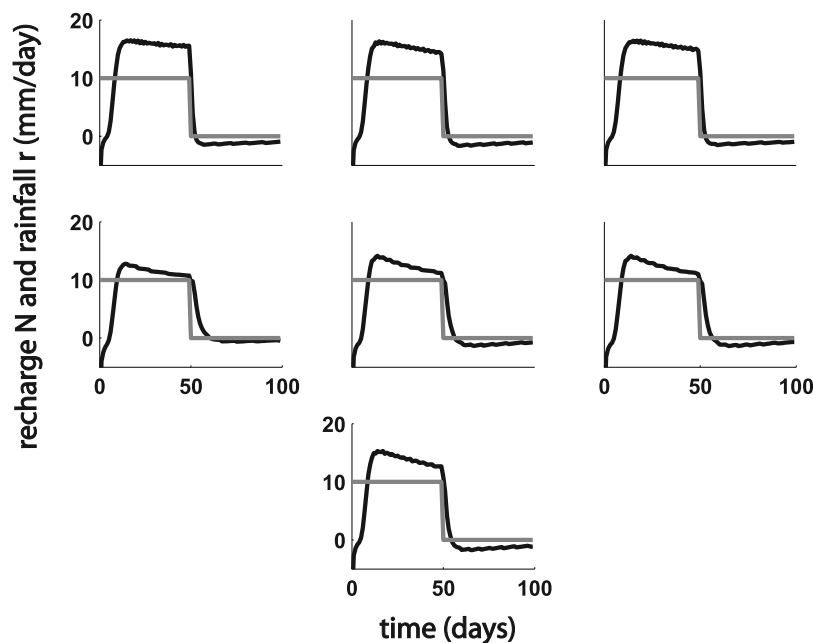


Figure 8. Rainfall rates (gray lines) and recharge rates (black lines) calculated using equation (16).

of capillarity become more prominent and conductivities decrease, the validity of the Boussinesq assumptions become increasingly questionable.

[44] The developed HSB coupled model is an efficient, parsimonious model that can be used in investigations of variable source areas, which play an important role in the generation of saturated overland flow and floods. Because the described model also outputs pressure heads and soil moisture contents in the unsaturated zone, it has potential applications in combination with land surface models, where unsaturated zone processes and interactions with shallow groundwater are generally not simulated well. Overall, the low dimensionality of the HSB model makes it appealing for poorly gauged catchments, since the required parameters are relatively easily accessible and since the model is much less computationally demanding than a full three-dimensional RE (or analogous) model. Future work includes testing the model in the field, for instance on the experimental hillslope and small catchment described by *Brooks et al.* [2004, 2007], and accounting for hysteresis and macropore flow.

7. Conclusions

[45] In this work we have presented a coupling between the one-dimensional Richards equation for unsaturated flow and the one-dimensional hillslope-storage Boussinesq model (HSB) [*Troch et al.*, 2003] for lateral saturated flow along complex hillslopes. In the model we have included the capillary fringe in the Boussinesq flow domain, i.e., the aquifer depth was taken to be the sum of the water table height and the height of the capillary fringe, ψ_c . We assumed the fluxes in the unsaturated zone to be vertical, and in the saturated zone parallel to the underlying impervious bedrock (i.e., Dupuit-Forchheimer assumption). We assumed that an average soil moisture profile derived for the entire hillslope provides an adequate description of unsat-

urated zone processes. This assumption, which proves to yield sufficiently accurate results based on the timing of the hydrographs, together with the manner in which the HSB formulation is able to represent a three-dimensional soil mantle as a one-dimensional flow system, makes possible a very efficient low-dimensional model of unsaturated and saturated hillslope dynamics.

[46] The role of the unsaturated zone in transmitting the soil moisture pulses as a result of rainfall is investigated, and the relationships between rainfall, recharge, drainable porosity and unsaturated storage are analyzed. Besides the expected delaying effect of the unsaturated zone on recharge rates, the simulations also showed that the unsaturated zone does not always dampen the rainfall signal, but can also amplify it, causing recharge rates to exceed rainfall rates under certain conditions. This effect is caused by water tables including water from the unsaturated zone into the saturated zone as they rise.

[47] The coupled model (HSB coupled) was compared (in terms of hydrographs and water table distributions) to the original HSB model (HSB original) and to a three-dimensional RE model (taken to be the benchmark) on a set of seven synthetic hillslopes, ranging from convergent to divergent. The modeled outflow rates of HSB original are systematically lower than those of the RE model. For the HSB coupled model, the outflow rates and the timing of the hydrographs (the time to the first increase in outflow, the time to peak, etc.) very closely matched that of the RE model for all hillslopes at all times. Also the match to the water tables is significantly better than that of HSB original, especially for the divergent slopes. The correct timing of the HSB coupled hydrographs suggests that a single soil moisture profile suffices to describe the unsaturated zone dynamics. We conclude that for the hillslope configurations and scenarios examined in this paper it is possible to reproduce hydrographs and water table dynamics with a good degree of accuracy.

[48] **Acknowledgments.** This work has been supported in part by Delft Cluster (project DC-030604). The authors also wish to thank John Selker and the reviewers for their very helpful comments.

References

- Abbott, M., J. Bathurst, J. Cunge, P. O'Connell, and J. Rasmussen (1986), An introduction to the European Hydrological System—Système Hydrologique Européen, "SHE," 1: History and philosophy of a physically-based, distributed modelling system, *J. Hydrol.*, *87*, 45–59.
- Abdul, A., and R. Gillham (1989), Field studies on the effects of the capillary fringe on streamflow generation, *J. Hydrol.*, *112*, 1–18.
- Barry, D., S. Barry, and J.-Y. Parlange (1996), Capillary correction to periodic solution of the shallow flow approximation, in *Mixing in Estuaries and Coastal Seas, Coastal Estuarine Stud.*, vol. 50, edited by C. Pattiaratchi, pp. 496–510, AGU, Washington, D. C.
- Bear, J. (1972), *Dynamics of Fluids in Porous Media*, Elsevier, New York.
- Berkowitz, B., S. Silliman, and A. Dunn (2004), Impact of the capillary fringe on local flow, chemical migration, and microbiology, *Vadose Zone J.*, *3*, 534–548.
- Beven, K. (1982), On subsurface stormflow: Prediction with simple kinematic theory for saturated and unsaturated flows, *Water Resour. Res.*, *18*, 1627–1633.
- Beven, K., and M. Kirkby (1979), A physically based variable contributing area model of basin hydrology, *Hydrol. Sci. Bull.*, *24*(1), 43–69.
- Boussinesq, J. (1877), Essai sur la thorie des eaux courantes, *Mem. Acad. Sci. Inst. Fr.*, *23*, 680 pp.
- Brooks, E., J. Boll, and P. McDaniel (2004), A hillslope-scale experiment to measure lateral saturated hydraulic conductivity, *Water Resour. Res.*, *40*, W04208, doi:10.1029/2003WR002858.
- Brooks, E., J. Boll, and P. McDaniel (2007), Distributed and integrated response of a geographic information system-based hydrologic model in the eastern Palouse region, *Hydrol. Processes*, *21*(1), 110–122, doi:10.1002/hyp.6230.
- Brutsaert, W. (1994), The unit response of groundwater outflow from a hillslope, *Water Resour. Res.*, *30*, 2759–2763.
- Chapman, T. (2005), Recharge-induced groundwater flow over a plane sloping bed: Solutions for steady and transient flow using physical and numerical models, *Water Resour. Res.*, *41*, W07027, doi:10.1029/2004WR003606.
- Childs, E. (1971), Drainage of groundwater resting on a sloping bed, *Water Resour. Res.*, *7*, 1256–1263.
- Duffy, C. (1996), A two-state integral-balance model for soil moisture and groundwater dynamics in complex terrain, *Water Resour. Res.*, *32*, 2421–2434.
- Dunne, T., and R. Black (1970), An experimental investigation of runoff production in permeable soils, *Water Resour. Res.*, *6*, 478–489.
- Freeze, R. (1972), Role of subsurface flow in generating surface runoff: 1. Base flow contributions to channel flow, *Water Resour. Res.*, *8*, 609–623.
- Gillham, R. (1984), The capillary fringe and its effect on water-table response, *J. Hydrol.*, *67*, 307–324.
- Harr, M. (1962), *Groundwater and Seepage*, McGraw-Hill, New York.
- Hewlett, J., and A. Hibbert (1967), Factors affecting the response of small watersheds to precipitation in humid areas, in *Forest Hydrology*, edited by W. Sopper and H. Lull, pp. 275–290, Elsevier, New York.
- Hilberts, A., E. van Loon, P. Troch, and C. Paniconi (2004), The hillslope-storage Boussinesq model for spatially variable bedrock slope, *J. Hydrol.*, *291*, 160–173.
- Hilberts, A., P. Troch, and C. Paniconi (2005), Storage-dependent drainable porosity for complex hillslopes, *Water Resour. Res.*, *41*, W06001, doi:10.1029/2004WR003725.
- Hillel, D. (1980), *Applications of Soil Physics*, Elsevier, New York.
- Hooghoudt, S. (1947), Waarnemingen van grondwaterstanden voor de landbouw, *Versl. Tech. Bijeenkomsten 1-6*, Tech. Natuurw. Onderz., The Hague, Netherlands.
- Ivanov, V., E. Vivoni, R. Bras, and D. Entekhabi (2004), Catchment hydrological response with a fully distributed triangulated irregular network model, *Water Resour. Res.*, *40*, W11102, doi:10.1029/2004WR003218.
- Jayatilaka, C., and R. Gillham (1996), A deterministic-empirical model of the effect of the capillary fringe on near-stream area runoff: 1. Description of the model, *J. Hydrol.*, *184*, 299–315.
- Kim, C., and M. Bierkens (1995), A formula for computation of time-varying recharge of ground water—Comment, *J. Hydrol.*, *171*, 191–193.
- Kim, C., G. Salvucci, and D. Entekhabi (1999), Groundwater-surface water interaction and the climatic spatial patterns of hillslope hydrological response, *Hydrol. Earth Syst. Sci.*, *3*(3), 375–384.
- Koster, R., M. Suarez, A. Ducharme, M. Stieglitz, and P. Kumar (2000), A catchment-based approach to modeling land surface processes in a general circulation model, *J. Geophys. Res.*, *105*(D20), 24,809–24,822.
- Koster, R., M. Suarez, R. Higgins, and H. van den Dool (2003), Observational evidence that soil moisture variations affect precipitation, *Geophys. Res. Lett.*, *30*(5), 1241, doi:10.1029/2002GL016571.
- Liang, X., Z. Xie, and M. Huang (2003), A new parameterization for surface and groundwater interactions and its impact on water budgets with the variable infiltration capacity (VIC) land surface model, *J. Geophys. Res.*, *108*(D16), 8613, doi:10.1029/2002JD003090.
- Luthin, J., and P. Day (1955), Lateral flow above a sloping water table, *Soil Sci. Soc. Am. Proc.*, *19*, 406–410.
- Luthin, J., and R. Miller (1953), Pressure distribution in soil columns draining into the atmosphere, *Soil Sci. Soc. Am. Proc.*, *17*, 329–333.
- McGlynn, B., J. McDonnell, J. Seibert, and C. Kendall (2004), Scale effects on headwater catchment runoff timing, flow sources, and groundwater-streamflow relations, *Water Resour. Res.*, *40*, W07504, doi:10.1029/2003WR002494.
- Michiels, P., R. Hartmann, and E. de Strooper (1989), Subsurface water flow on a slope in the loamy region of Belgium, *Earth Surf. Processes Landforms*, *14*, 533–543.
- Nachabe, M. (2002), Analytical expressions for transient specific yield and shallow water table drainage, *Water Resour. Res.*, *38*(10), 1193, doi:10.1029/2001WR001071.
- Nielsen, P., and P. Perrochet (2000), Watertable dynamics under capillary fringes: Experiments and modelling, *Adv. Water Resour.*, *23*, 503–515.
- O'Loughlin, E. (1981), Saturation regions in catchments and their relations to soil and topographic properties, *J. Hydrol.*, *53*, 229–246.
- Paniconi, C., and M. Putti (1994), A comparison of Picard and Newton iteration in the numerical solution of multidimensional variably saturated flow problems, *Water Resour. Res.*, *30*, 3357–3374.
- Paniconi, C., and E. Wood (1993), A detailed model for simulation of catchment scale subsurface hydrological processes, *Water Resour. Res.*, *29*, 1601–1620.
- Paniconi, C., P. Troch, E. van Loon, and A. Hilberts (2003), Hillslope-storage Boussinesq model for subsurface flow and variable source areas along complex hillslopes: 2. Intercomparison with a three-dimensional Richards equation model, *Water Resour. Res.*, *39*(11), 1317, doi:10.1029/2002WR001730.
- Parlange, J. Y., and W. Brutsaert (1987), A capillarity correction for free surface of groundwater, *Water Resour. Res.*, *23*, 805–808.
- Parlange, J. Y., W. Brutsaert, J. Fink, and A. El-Kadi (1990), A capillarity correction for free surface flow revisited, *Water Resour. Res.*, *26*, 1691–1692.
- Pikul, M., R. Street, and I. Remson (1974), A numerical model based on coupled one-dimensional Richards and Boussinesq equations, *Water Resour. Res.*, *10*, 295–302.
- Putti, M., and C. Paniconi (2004), Time step and stability control for a coupled model of surface and subsurface flow, in *Computational Methods in Water Resources*, vol. 2, edited by C. Miller et al., pp. 1391–1402, Elsevier, New York.
- Reggiani, P., M. Sivapalan, and S. Hassanizadeh (1998), A unifying framework for watershed thermodynamics: Balance equations for mass, momentum, energy and entropy, and the second law of thermodynamics, *Adv. Water Res.*, *22*(3), 367–398.
- Seibert, J., and J. McDonnell (2002), On the dialog between experimentalist and modeler in catchment hydrology: Use of soft data for multicriteria model calibration, *Water Resour. Res.*, *38*(11), 1241, doi:10.1029/2001WR000978.
- Sloan, W. (2000), A physics-based function for modeling transient groundwater discharge at the watershed scale, *Water Resour. Res.*, *36*, 225–241.
- Smith, R., and R. Hebbert (1983), Mathematical simulation of interdependent surface and subsurface hydrologic processes, *Water Resour. Res.*, *19*, 987–1001.
- Szilagy, J., M. Parlange, and J. Albertson (1998), Recession analysis for aquifer parameter determination, *Water Resour. Res.*, *30*, 1851–1857.
- Torres, R., W. Dietrich, D. Montgomery, S. Anderson, and K. Loague (1998), Unsaturated zone processes and the hydrologic response of a steep, unchanneled catchment, *Water Resour. Res.*, *34*, 1865–1879.
- Troch, P. (1992), Conceptual basin-scale runoff process models for humid catchments: Analysis, synthesis and applications, Ph.D. thesis, Ghent Univ., Brussels.
- Troch, P., E. van Loon, and A. Hilberts (2002), Analytical solutions to a hillslope-storage kinematic wave equation for subsurface flow, *Adv. Water Resour.*, *25*, 637–649.
- Troch, P., C. Paniconi, and E. van Loon (2003), Hillslope-storage Boussinesq model for subsurface flow and variable source areas along complex

- hillslopes: 1. Formulation and characteristic response, *Water Resour. Res.*, 39(11), 1316, doi:10.1029/2002WR001728.
- Vachaud, G., and M. Vauclin (1975), Comment on "A numerical model based on coupled one-dimensional Richards and Boussinesq equations" by Mary F. Pikul, Robert L. Street, and Irwin Remson, *Water Resour. Res.*, 11, 506–509.
- van Genuchten, M. (1980), A closed-form equation for predicting the hydraulic conductivity of unsaturated soils, *Soil Sci. Am. J.*, 44, 892–898.
- Weiler, M., and J. McDonnell (2004), Virtual experiments: A new approach for improving process conceptualization in hillslope hydrology, *J. Hydrol.*, 285, 3–18.
- Wigmosta, M., L. Vail, and D. Lettenmaier (1994), A distributed hydrology-vegetation model for complex terrain, *Water Resour. Res.*, 30, 1665–1679.
- Wood, E., D. Lettenmaier, and V. Zartarian (1992), A land-surface hydrology parameterization with subgrid variability for general circulation models, *J. Geophys. Res.*, 97(D3), 2717–2728.
- Woods, R., M. Sivapalan, and J. Robinson (1997), Modeling the spatial variability of subsurface runoff using topographic index, *Water Resour. Res.*, 33, 1061–1073.
-
- J. Boll, Department of Biological and Agricultural Engineering, University of Idaho, Moscow, ID 83844, USA. (jboll@uidaho.edu)
- A. G. J. Hilberts, Climate Hazard Model Development, Risk Management Solutions Ltd., Peninsular House, 30 Monument Street, London EC3R 8HB, London, UK. (arno.hilberts@gmail.com)
- C. Paniconi, Centre Eau, Terre et Environnement, Institut National de la Recherche Scientifique, Université du Québec, 490 de la Couronne, Québec, QC, Canada G1K9A9. (claudio_paniconi@ete.inrs.ca)
- P. A. Troch, Department of Hydrology and Water Resources, University of Arizona, 1122 East North Campus Drive, Harsbarger Building, P.O. Box 210011, Tucson, AZ 85721, USA. (patroch@hwr.arizona.edu)